Universiteit Utrecht

Opleiding Natuur- en Sterrenkunde

Effect of turbulence modelling, light intensity and tidal flow on phytoplankton in estuaries

Bachelor Thesis

Bouke Biemond

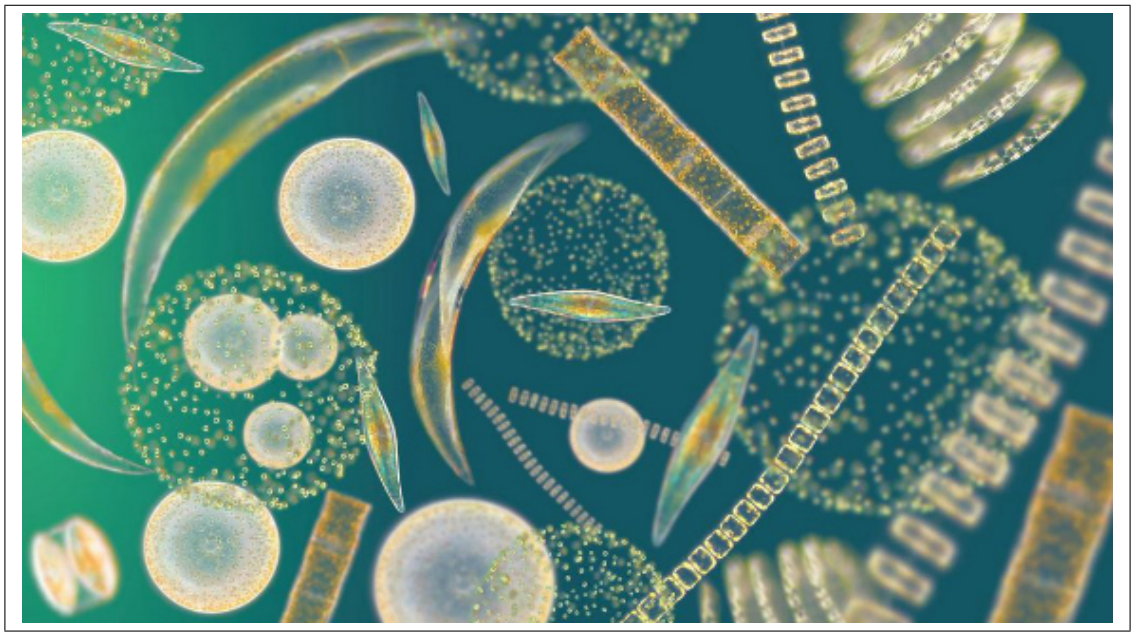

Supervisors:

Prof. dr. H.E. de Swart
IMAU

dr. E. van Sebille
IMAU

June 13, 2018

Abstract

This study focusses on hydrodynamics and phytoplankton dynamics in estuaries, the transition areas between rivers and seas. Gaining insight into phytoplankton behaviour, in particular the formation of blooms, is important to improve management of estuaries. For this, both complex numerical models as well as idealised models are employed. In this study, an existing idealised numerical model is extended to gain knowledge about the influence of several factors on the phytoplankton blooms in well-mixed (i.e. salinity does not vary in the vertical direction) estuaries.

The formulation of turbulent vertical exchange processes, as represented by the vertical eddy viscosity (A_ν) and vertical eddy diffusivity (κ_ν) is the first factor investigated. Here, κ_ν and A_ν are given a parabolic distribution in the vertical, instead of keeping it constant. The observed differences with the reference experiments are small, about 1 %. The most remarkable difference is that a lower equilibrium phytoplankton concentration is found, which is explained by the development of a lower nutrient concentration in the first weeks of the experiment, which causes less growth in the first weeks.

The second factor that was modified is the light intensity: it was given a diurnal variation, with the same mean value as in the original model, instead of keeping it constant in time. This results in a lower phytoplankton concentration, which is explained by the fact that phytoplankton is normally limited by nutrients, but due to the low light intensity at night there is an extra limitation on the growth.

By combining these two factors, the effect caused by the diurnal light cycle dominates. No additional effects are observed.

The last influence investigated is the role of involving explicit tidal flow in these well-mixed estuaries. A time-dependent velocity profile was used to model the tidal flow. The model did not work with these settings: the tidal flow flushed most of the nutrients to the sea what prevented a phytoplankton bloom from occurring. Analysis demonstrated that the addition of tidal flow requires proper adjustments of the conditions imposed at the seaward boundary.

Contents

1 Introduction

This study will focus on spatial patterns of phytoplankton blooms in estuaries. In this introduction, first the relevance of this study is described, followed by a brief summary of the existing knowledge, and by the research questions.
An estuary is a semi-enclosed body of water (a picture of an example of this is placed in figure 1) where fresh water from a river mixes with the salty seawater. The main source of this mixing is turbulent mixing, which in most cases is generated by tidal currents moving over a rough bottom[*Dyer*, 1997]. Estuaries are an important part of the earth. Many cities are built close to estuaries, for example Dhaka, Hamburg, New Orleans, Rotterdam, Shanghai, London, because of the fertile grounds and opportunities for trade and fishing. So, a lot of economic activity takes place there.
"Phytoplankton" is a different word for "microscopic marine algae"[*NOAA*, 2017]. They are an important part of the marine ecosystem. They play a role similar to the role plants play on the land, because they use photosynthesis to grow, and are at the bottom of the food chain in all almost every ocean, sea, river and lake [*NASA*, 2010], just like plants on the land.
In order to gain knowledge about the biology of estuaries, it is very important to understand the behaviour of phytoplankton. And the biology of the estuaries is important for the large numbers of people who live close to them. For example, phytoplankton blooms, as investigated in this study, can be harmful, for instance when a toxic species is growing, or the phytoplankton uses all the present oxygen in the water.

There have been several studies to phytoplankton in estuaries in the past. One can distinguish them in three groups: observational, complex simulation models and idealised simulation models. Observational studies use field data and statistics to study phytoplankton. Complex simulation models use mathematical models, which are applied to one estuary. Their goal is to reproduce the measurements in one specific estuary as detailed as possible. Idealised simulation models are mathematical models too, but are not focussed on one estuary, but are developed to investigate which factors are influencing the phytoplankton.
First some observational studies will be discussed. *Sin et al.* [1999] investigated phytoplankton patterns in the York estuary (which is located at the east coast of the USA), and found a relation between the river discharge and the location of the phytoplankton blooms: low river discharge made the plankton bloom shift landwards. *Maier* [2012] found that phytoplankton blooms occur during low river discharge in the Taw estuary(located in South-West England). Finally, *Carstensen et al.* [2015] used field data of several estuaries, and reported that phytoplankton blooms formed in spring form earlier in estuaries with a high light intensity compared to estuaries with a low light intensity. They suggest that the reason for this behaviour is that phytoplankton blooms are triggered by a rising water temperature or light incidence.
Using a complex simulation model, *Azevedo et al.* [2014] found that, in the Douro estuary (located in Portugal), there is a parabolic relation between river discharge and total amount of phytoplankton in the estuary, with a maximum

Figure 1: The Taw estuary in England.

for moderate river discharge. *Naithani et al.* [2016] used a complex model, with taking into account varying light intensity, to study phytoplankton in the Scheldt estuary(located in the Netherlands). They demonstrated that river discharge plays an important role in phytoplankton blooms in the Scheldt estuary too: high river discharge means a lot of turbidity, which lowers the light intensity, and low river discharge means less supply of nutrients.
To better identify the mechanisms that are responsible for this dependence of phytoplankton on river discharge, *Liu and de Swart* [2015] built an idealised model. They found that the observed spatial patterns in phytoplankton blooms can be explained as follows: In the upper reach (i.e. the part which is closest to the river) of the estuary, plankton grows fast because of the high nutrient concentration here (nutrients in an estuary are predominantly supplied by the river flow). In the lower reach hardly any phytoplankton grows due to the absence of nutrients. That is one important factor which causes patterns in the longitudinal direction. The other factor accounting for spatial variation in this direction is the river flow: it advects phytoplankton and nutrients to the lower reach. So, for low river discharge (and thus low flow velocities in the river) the phytoplankton bloom will occur in the upper reach. For moderate river discharge, the bloom will shift to the middle of the estuary. For high river discharge, no phytoplankton bloom will take place in the estuary because the phytoplankton flows fast to the sea.

The model of *Liu and de Swart* [2015] is highly idealised. One limitation is that is assumes time and space independent vertical eddy viscosity and vertical eddy diffusivity. This is however an approximation. A more realistic choice is giving the eddy diffusivity and eddy viscosity constants a parabolic distribution over the vertical, as suggested by *Burchard and Hetland* [2010]. Another assumption is that it takes the light intensity constant. Moreover, only subtidal currents are accounted for in the model, so tides only act as a source of turbulence. But in reality, these tides make the flow in an estuary highly time-dependent, which can lead to additional net transports of phytoplankton and nutrients.

The previous considerations motivate the four main questions of this study:

- What is the influence of a parabolic distribution over the depth of vertical eddy viscosity and of vertical eddy diffusivity on the timing, location, size and vertical structure of the phytoplankton blooms?
- What is the influence of diurnal varying light intensity on the timing, location, size and vertical structure of the phytoplankton blooms?
- What is the influence of taking into account both varying light intensity and a parabolic distribution of the eddy viscosity and eddy diffusivity on the timing, location, size and vertical structure of the phytoplankton blooms?
- What is the influence of including explicit tidal flow on the timing, location, size and vertical structure of the plankton blooms?

In section 2, the used method is described. Section 3 presents the results. These results are analysed and discussed in section 4. Finally, conclusions are given in section 5.

2 Methodology

In this study, an extension of the phytoplankton model of *Liu and de Swart* [2015] is used, which will be described in section 2.1. After that it is specified what is modified in this model in order to answer the research questions.

2.1 The model

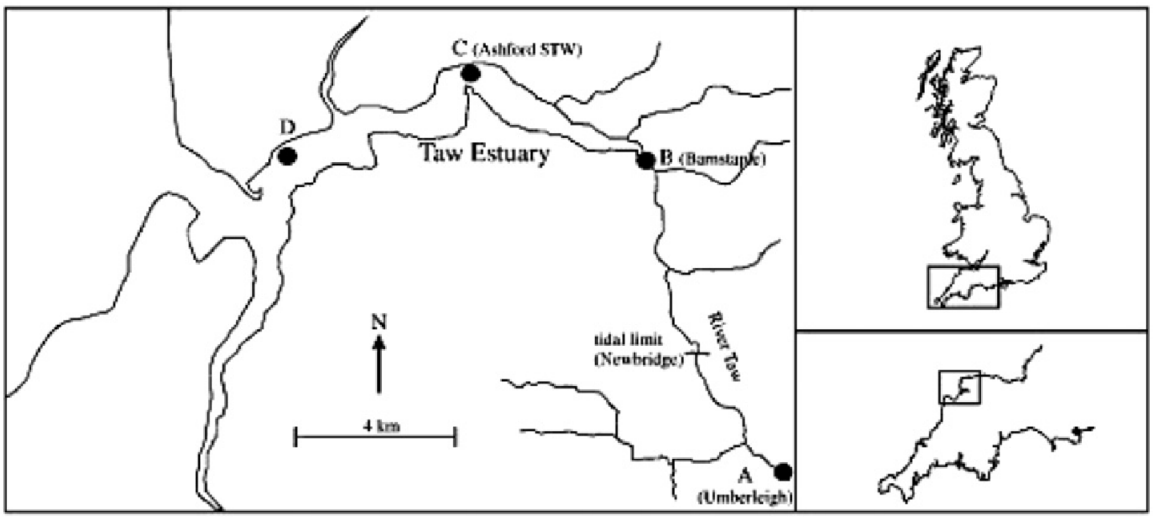

Figure 2: The location of the Taw estuary (this figure is taken from *Maier* [2012]). The circles A-D are sampling sites, used by *Maier* [2012]

The model of *Liu and de Swart* [2015] is an idealised model. For this case it takes the Taw estuary in England as an example, because this estuary is well-mixed in the vertical, and the model results can be compared with the field data

of *Maier* [2012]. A figure of the location and shape of this estuary is placed in figure 2. A two-dimensional Cartesian grid is used to model the estuary (with an along-channel and a vertical coordinate). This situation is sketched in figure 3.

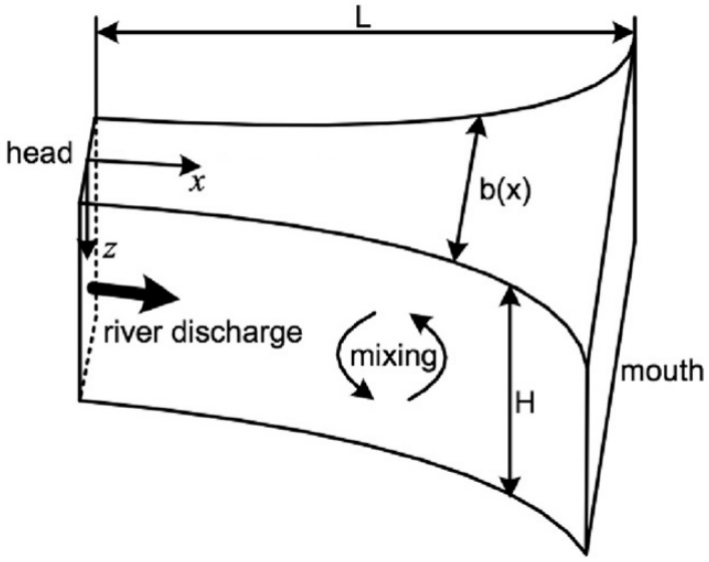

Figure 3: A sketch of the model.

The most important equations of this model are those of the rate of change of P and N. They read:

$$\frac{\partial P}{\partial t} = \mu(N,I)P - mP - \nu\frac{\partial P}{\partial z} - w\frac{\partial P}{\partial z} - u\frac{\partial P}{\partial x} + \frac{\partial}{\partial z}(\kappa_\nu\frac{\partial P}{\partial z}) + \frac{1}{b}\frac{\partial}{\partial x}(b\kappa_h\frac{\partial P}{\partial x}), \tag{1}$$

$$\frac{\partial N}{\partial t} = -\alpha\mu(N,I)P + \alpha\epsilon mP - w\frac{\partial N}{\partial z} - u\frac{\partial N}{\partial x} + \frac{\partial}{\partial z}(\kappa_\nu\frac{\partial N}{\partial z}) + \frac{1}{b}\frac{\partial}{\partial x}(b\kappa_h\frac{\partial N}{\partial x}), \tag{2}$$

$$\mu(N,I) = \mu_{max}\min(\frac{N}{H_N+N}, \frac{I}{H_I+I}), \tag{3}$$

$$I = I_{in}\exp(-k_{bg}z - k_{phyto}\int_o^z P(t,\theta)d\theta), \tag{4}$$

$$\kappa_h(x) = \frac{Qs}{Hb\frac{ds}{dx}}. \tag{5}$$

Equation 1 describes the evolution of the phytoplankton concentration in time, equation 2 does the same for the nutrients in the estuary. Equation 3 describes the growth of the phytoplankton [*Huisman et al.*, 2006], and equation 4 is the Lambert-Beer law, which describes how much light penetrates the water. Finally, equation 5 calculates the longitudinal turbulent diffusivity [*Helder and Ruardij*,

1982] In these equations x is the along-channel coordinate, with corresponding velocity u, and z is the vertical coordinate with corresponding velocity w. In both cases, the unit of the coordinate is meters and the unit of the velocities is meter/second. The character used for time is t, and it is given in seconds. The meaning of the other symbols is specified in table 1.

These equations need boundary conditions, to be solvable. They are in this case:

$$(\nu P - \kappa_\nu \frac{\partial P}{\partial z})\Big|_{z=0,z=H} = 0, \quad (6) \qquad (\kappa_\nu \frac{\partial N}{\partial z})\Big|_{z=0,z=H} = 0, \quad (7)$$

$$(uP - \kappa_h \frac{\partial P}{\partial x})\Big|_{x=0} = 0, \quad (8) \qquad N\Big|_{x=0} = N_{river}, \quad (9)$$

$$P\Big|_{z=0} = P_{sea}, \quad (10) \qquad N\Big|_{z=0} = N_{sea}. \quad (11)$$

The meaning of the used constants can again be found in table 1.

What is also needed to know to get the model working, are the velocities in de longitudinal and vertical direction. They are calculated by solving the following equations:

$$0 = -\frac{1}{\rho_0}\frac{\partial p}{\partial x} + \frac{\partial}{\partial z}(A_\nu \frac{\partial u}{\partial z}), \quad (12)$$

$$\frac{\partial p}{\partial z} = -\rho g, \quad (13)$$

$$\frac{\partial u}{\partial x} + \frac{\partial w}{\partial z} = 0, \quad (14)$$

$$\rho = \rho_0 + \beta s, \quad (15)$$

$$s(x) = \frac{1}{2} s_* \Big(1 + \tanh(\frac{x - x_c}{x_L})\Big). \quad (16)$$

Equation 12 is the horizontal momentum balance, 13 is the hydrostatic balance and equation 14 is the continuity equation. Equation 15 is the equation of state. Equation 16 models the salinity profile in the estuary [*Warner et al.*, 2005]. The meaning of the used symbols is explained in table 1.

All these equations combined give the evolution of P and N in time, for every grid point of the estuary. To solve these differential equations, a finite difference method is used for the advection and diffusion terms, and a fourth-order Runge-Kutta scheme is used for the time derivates.

The output of this model is for every time and at every position (in two dimensions, the cross-stream coordinate is not taken into account) the phytoplankton and nutrient concentration. On top of that, the output of the model

Symbol	Meaning	Dimension	Value (if relevant)
P	phytoplankton concentration	cells m^{-3}	n/a
N	nutrient concentration	mmol m^{-3}	n/a
μ	growth rate of phytoplankton	s^{-1}	n/a
I	light intensity	µmol photons m^{-2} s^{-1}	n/a
m	loss of phytoplankton	day^{-1}	0.24 (a)
ν	sinking velocity of plankton due to gravity	m day^{-1}	1.0 (a)
κ_ν	vertical turbulent diffusivity coefficient	m^2 s^{-1}	6×10^{-3}
b	estuarine width	m	n/a
κ_h	longitudinal turbulent diffusivtiy coefficient	m^2 s^{-1}	n/a
α	nutrient amount in each phytoplankton cell	mmol nutrient $cell^{-1}$	1×10^{-9} (b)
ϵ	part of respired/grazed phytoplankton that is recycled	dimensionlessf	0.5 (b)
μ_{max}	maximum growth rate	day^{-1}	0.96 (c)
H_N	half-saturation constant for nutrient-limited growth	mmol nutrient m^{-3}	0.5 (a)
H_I	half-saturation constant for light-limited growth	µmol photons $m^{-2}s^{-1}$	20 (b)
I_{in}	incident light intensity	µmol photons m^{-2} s^{-1}	400
k_{bg}	background turbidity	m^{-1}	0.045 (d)
k_{phyto}	light absorption by phytoplankton	m^2 $cell^{-1}$	6×10^{-10} (d)
θ	integration dummy variable	m	n/a
Q	river discharge	m^3 s^{-1}	n/a
H	depth of the estuary	m	7 (e)
g	gravitational acceleration	m s^{-2}	9.81
β	coefficient of isohaline concentration	kg m^{-3} psu^{-1}	0.83
ρ_0	reference density	kg m^{-3}	10^3
A_v	vertical eddy viscosity	m^2 s^{-1}	6×10^{-3}
s	salinity	psu	n/a
s_*	seawater salinity	psu	34 (f)
x_c	position where the salinity is 0.5 s_*	m	n/a
x_L	width of the salinity front	m	n/a
N_{river}	nutrient value in the river	mmol m^{-3}	2.5 (f)
N_{sea}	nutrient value in the sea	mmol m^{-3}	0.25 (f)
P_{sea}	plankton concentration in the sea	cells/m^{-3}	10^7 (g)
L_b	e-folding length scale of the estuary width	m	5300 (e)

Table 1: Explanation of the symbols used in 2.1. The sources for the used constants are: (a)*Sarthou et al.* [2005], (b) *Huisman et al.* [2006], (c) *Popovich and Gayoso* [1999], (d) *May et al.* [2003], (e) *Pethick* [2007], (f) *Maier* [2012] and (g) *Dugdale et al.* [2012]

gives the value of every term in equations 1 and 2. This gives the possibility to study the dynamics of phytoplankton in an estuary.
It is stressed that the description of model is short. More details are given in *Liu and de Swart* [2015].

2.2 Design of the experiments related to the first research question

To answer the first research question, it is needed to involve the parabolic distribution of A_ν and κ_ν in the equations (A_ν equals κ_ν, because there is no stratification in the vertical [*Munk and Anderson*, 1948]). This changes equations 1 and 2, and the flow velocities will become different too.

The parabolic distribution we used for the vertical turbulent diffusivity coefficient is parametrised by the following formula [*Fischer*, 1979]:

$$A_\nu(z) = \kappa_\nu(z) = \alpha z(H - z). \tag{17}$$

The profile of A_ν is plotted in figure 4. Here, α is a constant with the value of $7.5 \times 10^{-4} s^{-1}$, and is chosen so that the mean value of A_v is the same as it was in the reference case of *Liu and de Swart* [2015].

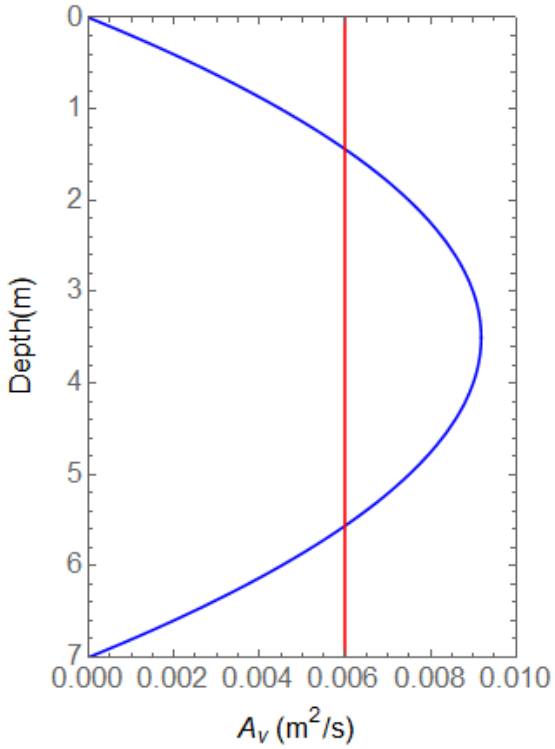

Figure 4: The profile of the vertical eddy diffusivity and eddy viscosity in the vertical. The red line represents the reference case, and the blue line represents the new profile of A_ν.

To include the new profile of κ_ν, changing the input of the input of the model is sufficient.
For the velocity profile, equations 12 up to and including 16 have to be solved. For the reference case, A_ν is taken constant. The calculation of the resulting velocities

is presented in *Hansen and Rattray* [1965](and is also used by *Liu and de Swart* [2015]).

To get the new profile of the velocity in the x-direction, the equations of motion have been solved again, with this new formulation of A_ν. This gives (for details see Appendix A):

$$u(x,t) = \frac{Q}{bH}\frac{\log(\frac{H-z}{z_0})}{\log(\frac{H}{z_0})-1+\frac{z_0}{H}} + \frac{gHB}{2\alpha\rho_0}\frac{ds}{dx}\left(1-\frac{z}{H}-\frac{z_0}{H}-\frac{(H-z_0)^2}{2H^2}\frac{(\log(\frac{H-z}{z_0})}{\log(\frac{H}{z_0})-1+\frac{z_0}{H}}\right). \tag{18}$$

The meaning of the used symbols is explained in table 1. One new symbol is introduced: z_0. This is the so-called roughness length, and is defined as the distance from the bottom at which the velocity becomes zero (and has obviously the dimension of meters). The typical value of this constant is z_0= 0.01 m.

The vertical velocity is calculated from the continuity equation (14), while using the new longitudinal velocity $u(x,t)$. The expression for $w(x,z)$ is not given here, because it is complicated and not very illuminating. Both these velocity profiles are plotted in figure 5.

Finally, the river discharge should be specified. For the Taw, the average river discharge is 10 m^3 s^{-1} [*Maier*, 2012]. So, one experiment is done, with Q=10 m^3 s^{-1}, and one reference experiment (where A_ν and κ_ν have the constant value of 6 $\times$ 10^{-3} m^2 s^{-1}).

The output of the model are values of the phytoplankton and nutrient concentration on each grid point on every day. A Wolfram Mathematica code is used to make plots of these results, so these results are visualised and suitable for further analysis.

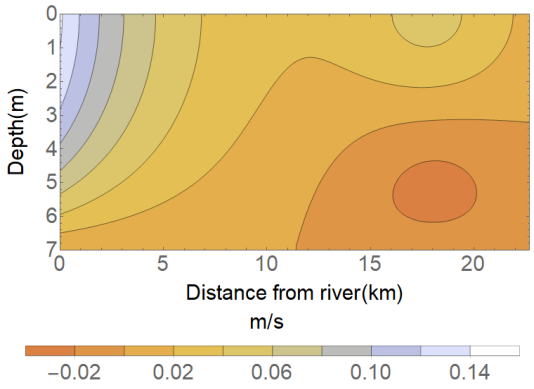

(a) The velocities in the x-direction for the reference experiment, so with a constant value for A_ν, for a river discharge of 10 m^3 s^{-1}.

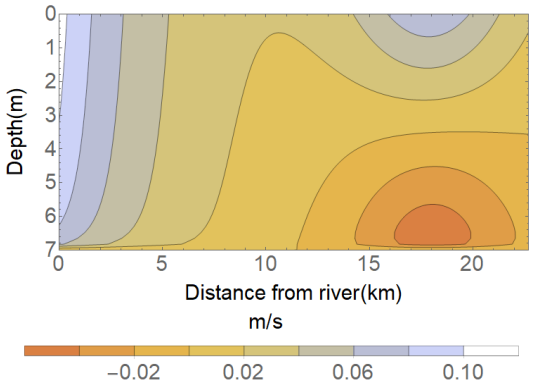

(b) The velocities in the x-direction for the experiment, so with a parabolic distribution of A_ν, for a river discharge of 10 m^3 s^{-1}.

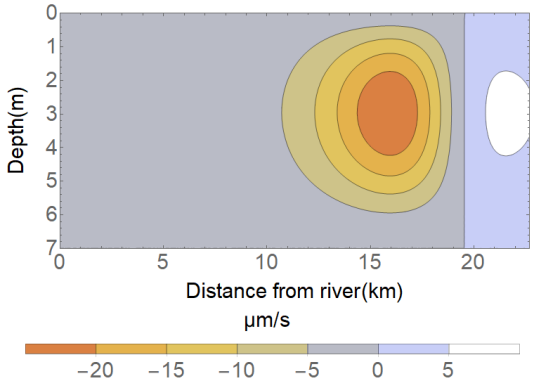

(c) As (a), but for the vertical velocity.

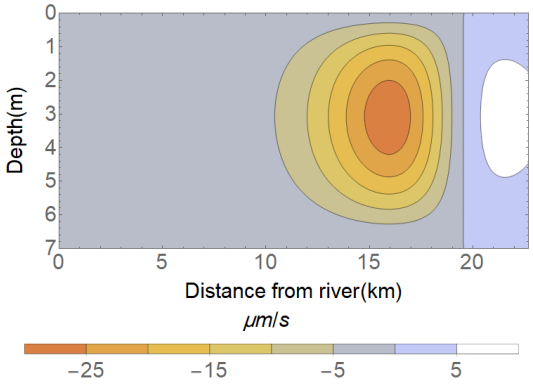

(d) As (b), but for the vertical velocity.

Figure 5: The velocities for the reference experiment and the experiment. Note the different meaning of the colours for the different figures.

2.3 Design of the experiments related to the second research question

To include varying light intensity, equation 4 should be modified. A cosine function was chosen to model the varying light intensity. This is not a fully realistic pattern for a diurnal cycle, but it is an easy way to investigate the influence of varying light intensity on the phytoplankton blooms. The formula for light intensity becomes

$$I = (1 + \cos(\frac{2\pi}{T}t + \pi))I_{in} \exp(-k_{bg}z - k_{phyto}\int_o^z P(t,\theta)d\theta), \tag{19}$$

One new symbol is introduced: T. This is the duration of one day. It has the value of 86400, and the unit is seconds. This is the only thing changed in the model. Again, one experiment (and a reference experiment, the same as used for the first research question) was done, with a river discharge of 10 m^3 s^{-1}. The output was taken two times per day: at noon and at midnight. The same Wolfram Mathematica code is used to analyse the results.

2.4 Design of the experiments related to the third research question

Here the two parts changed in the first and second research question are both involved at the same time. So, to summarise, the differences with the reference experiments (they have the input values of *Liu and de Swart* [2015] for the corresponding amount of river discharge) are:

1. The light intensity is time-dependent, and calculated with equation 19.
2. The longitudinal velocity profile follows equation 18, and the vertical velocity is calculated with equation 14.
3. The vertical eddy diffusivity is calculated with equation 17.

As found in earlier studies [*Azevedo et al.*, 2014], river discharge is one of the most important factors influencing the phytoplankton blooms. So it was decided to conduct runs for different values of river discharge. The average river discharge(Q) of the Taw is 10 m^3 s^{-1}, with deviations ranging from 1 to 100 m^3 s^{-1}[*Maier*, 2012]. To get these variations, six experiments were done (and for every experiment a reference experiment with a constant light intensity and a constant profile of vertical eddy diffusivity and eddy viscosity in the vertical), with the following values for the river discharge: 1, 2, 5, 10, 20 and 50 m^3 s^{-1}, so the effect of the parabolic eddy viscosity and eddy diffusivity combined with varying light intensity on the different cases of river discharge could be studied. The output was taken two times per day: at noon and at midnight. The same Wolfram Mathematica code is used to analyse the results.

2.5 Design of the experiments related to the fourth research question

To involve the explicit flow, a tidal velocity profile was adopted from *Ensing et al.* [2015]. The velocity profiles are rather complicated, so they are presented in appendix B. Plots of the velocity profiles in the longitudinal direction are made for two points of time and placed in figure 2.5. These velocities are added to the velocity profiles of the reference case.

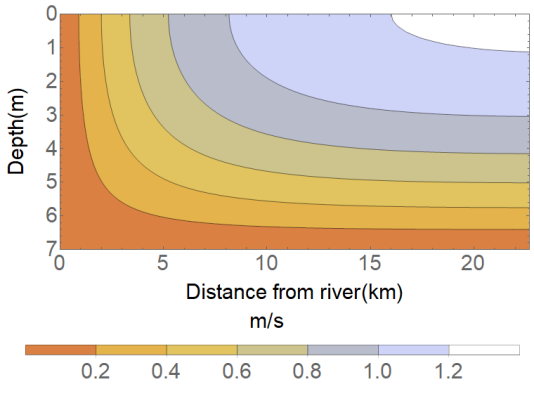

(a) The velocities in the x-direction, when there is a strong tidal flow to the sea.

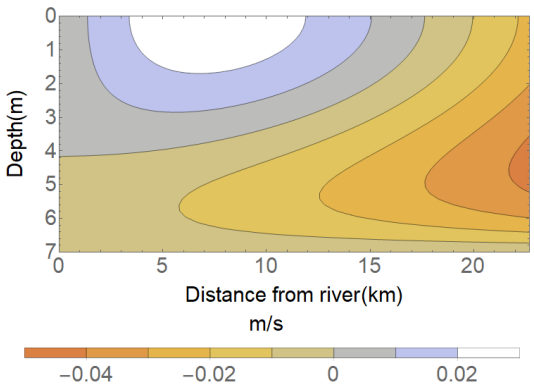

(b) As (a), but for a different time.

One experiment is done, with a river discharge of 10 m^3 s^{-1}. The reference experiment uses a time-independent velocity profile (and none of the modifications done to address the other research questions are executed). The output was taken

four times per day, to cover all stages of the tide (this gives the opportunity to take the mean value, what can be compared to the reference experiment). The same Wolfram Mathematica code is used to analyse the results.

3 Results

3.1 Reference experiment

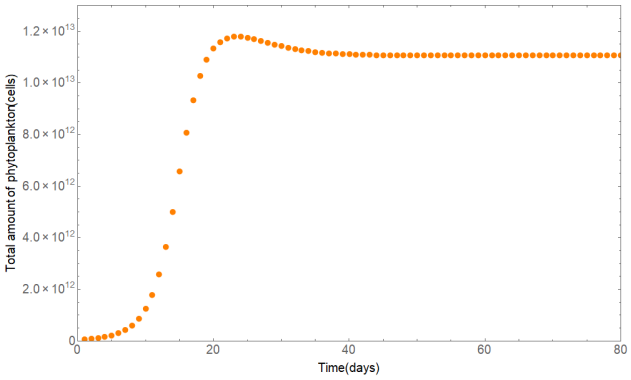

(a) The total amount of phytoplankton versus time.

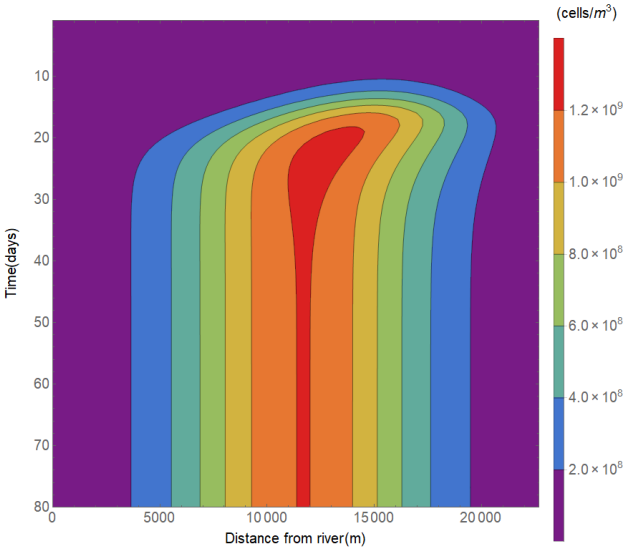

(b) The depth-averaged phytoplankton concentration, versus time and distance from the river.

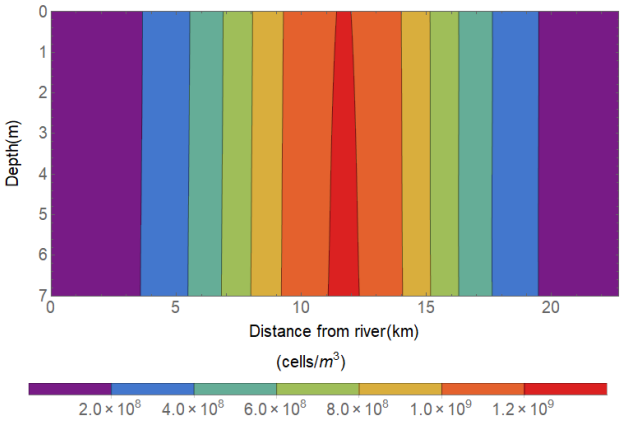

(c)The phytoplankton concentration on the 50th day, versus depth and distance from the river.

Figure 6: The results of the reference experiment (and Q=10 m^3 s^{-1}).

Figure 6(a) shows the time-evolution of the total amount of phytoplankton in the estuary. A phytoplankton bloom starts to grow and reaches his maximum value at the 24th day. Figure 6(b) shows the depth-averaged phytoplankton concentration, versus time and distance from river, so where in the estuary the phytoplankton blooms forms. The maximum value can be found around 12 kilometres from the river. Figure 6(c) illustrates the concentration phytoplankton versus distance

from river and depth on the 50th day of the simulation. This illustrates that no vertical structure in phytoplankton concentration arises .

3.2 Parabolic distribution of vertical eddy diffusivity and vertical eddy viscosity

Plots of the output of the model are made. These can be found in figure 7. Figures 7(a), (b) and (c) display the same results as figures 6(a), (b) and (c), but now for parabolic distribution of vertical edddy viscosity and vertical eddy diffusivity. Similar patterns as in the reference experiment are observed.

To give more insight in the differences between these experiments, figures were made which show the differences (between the experiment and the reference experiment) in these values. Figure 7(d) shows the difference in the total amount of phytoplankton versus time. One can see here that the size of the bloom is smaller for every point of time (this is a small difference, about 1%), and that the maximum deviation occurs a few days before the bloom reaches his maximum size. The day at which the bloom reaches his maximum size does not differ from the reference experiment.

Figure 7(e) shows the difference in the phytoplankton concentration versus time and distance from river. One can see that in the steady situation, there are two locations where a lower phytoplankton concentration is found: around 8 kilometres and around 16 kilometres from the river. Figure 7(f) illustrates the vertical structure of the phytoplankton on the 50th day. It is visible that the lower concentrations around 8 and 16 kilometres are predominantly present in the lower half of the estuary. The differences here are small too: around 1%. This is not enough to let the bloom significantly shift or cause a different structure in the vertical.

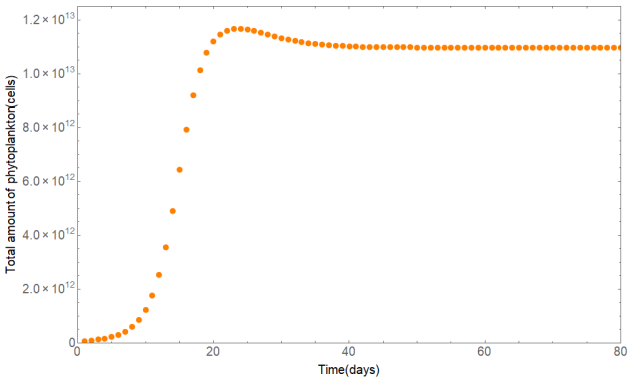

(a) The total amount of phytoplankton versus time.

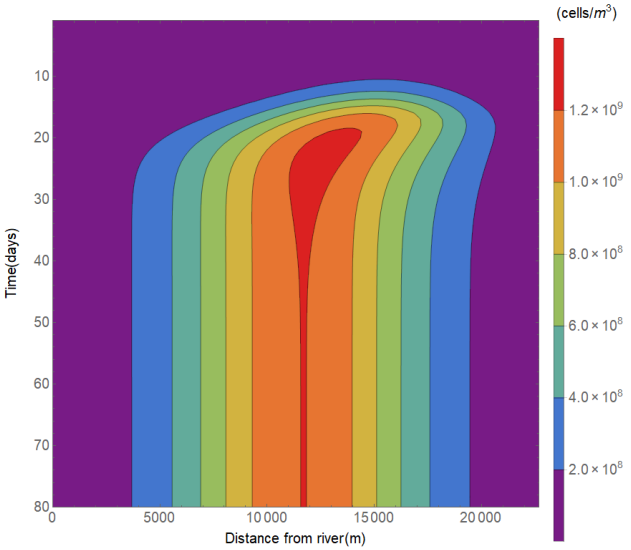

(b) The phytoplankton concentration averaged over the depth, versus depth and distance from the river.

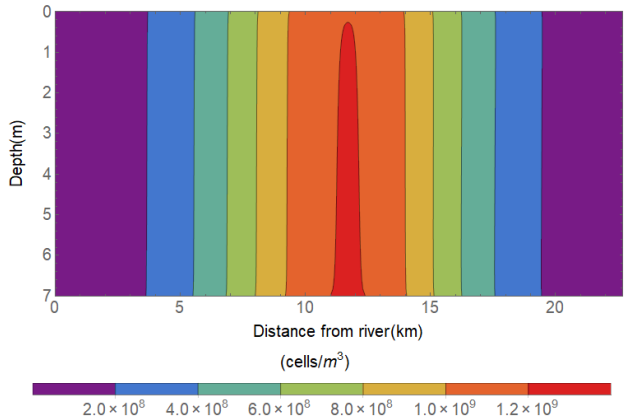

(c) The phytoplankton concentration on the 50th day, versus depth and distance from the river.

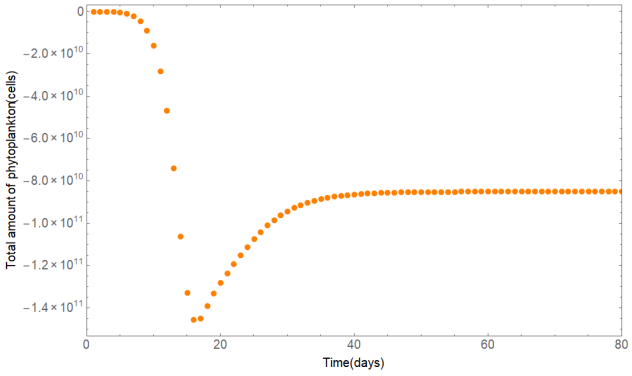

(d) As (a), but for the difference with the reference experiment.

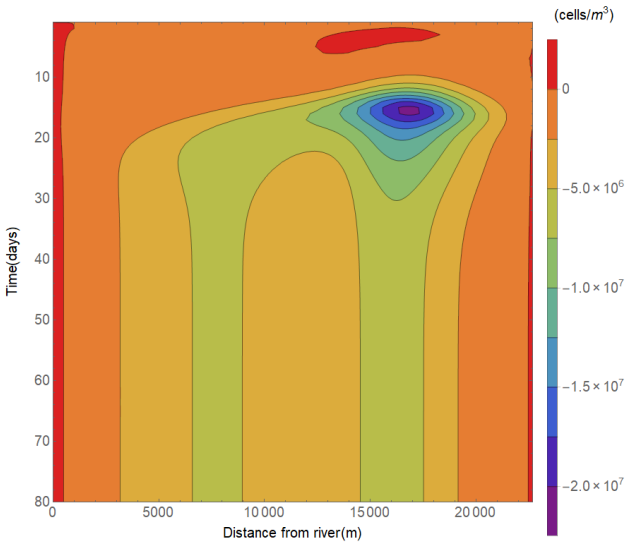

(e) As (b), but for the difference with the reference experiment.

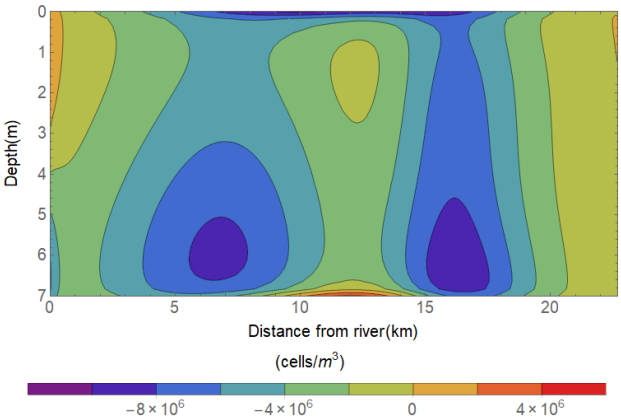

(f) As (c), but for the difference with the reference experiment.

Figure 7: The results of the experiment with a parabolic profile of the vertical eddy viscosity and vertical eddy diffusivity (and Q=10 m^3 s^{-1}).

3.3 Varying light intensity

Plots of the output of the model are made, where the average value is taken of values at noon and midnight, and placed in Figure 8. Figures 8(a), (b) and (c) display the same results as figures 6(a), (b) and (c), but now for a diurnal cycle of light intensity. The observed patterns are similar to those of the reference case. Comparing figure 8(a) with 6(a), it is visible that the timing of the bloom is changed: in the reference case the maximum amount of plankton occurs at the 24th day, while in the experiment with varying light intensity the maximum size of the phytoplankton blooms occurs at the 28th day.
Figure 8(d) illustrates the difference in the total amount of phytoplankton in the estuary, between the reference experiment and the experiment. One can see that the total amount of phytoplankton (and thus the size of the bloom) is smaller. The deviation is about 15%.
Figure 8(e) illustrates the difference in the phytoplankton concentration averaged over the depth, versus depth and distance from the river. One can see here that in the steady situation, the maximum deviation occurs around 9 kilometres from the river. After 15 kilometres more phytoplankton is found compared to the reference experiment. This makes the bloom shift seawards, what becomes even more clear when comparing figures 6(c) and 8(c): the maximum phytoplankton concentration in the reference experiment is found around 12 kilometres from the river mouth, but in the experiment it lays about 13 kilometres from the river mouth.

Figure 8(f) shows the difference in concentration phytoplankton versus distance from river and depth. It is visible that no vertical structure arises in this case.

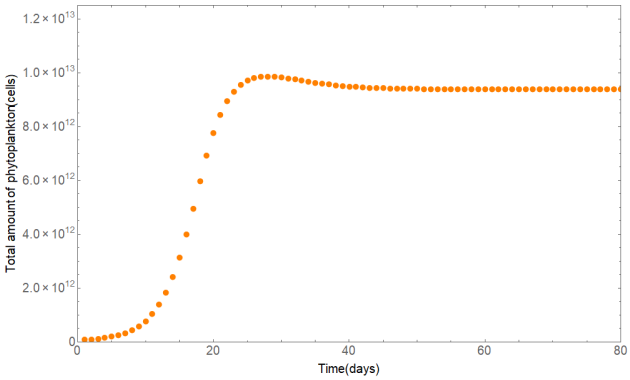

(a) The total amount of phytoplankton versus time.

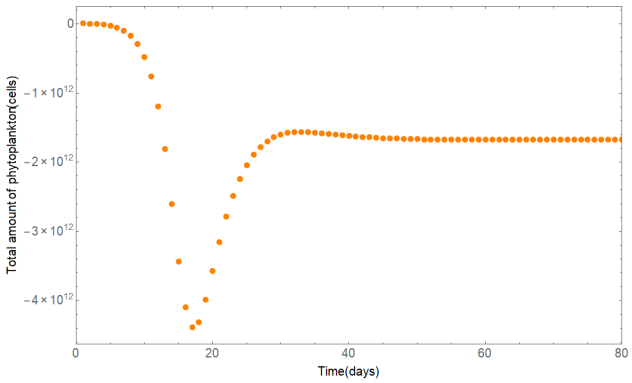

(d) As (a), but for the difference with the reference experiment.

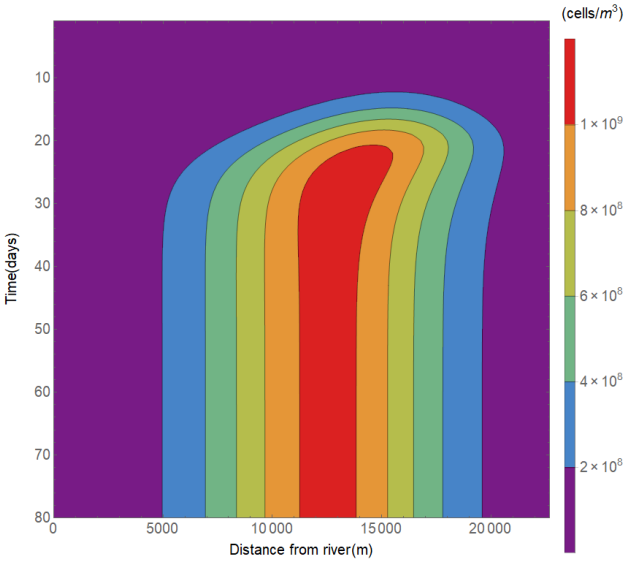

(b) The phytoplankton concentration averaged over the depth, versus depth and distance from the river.

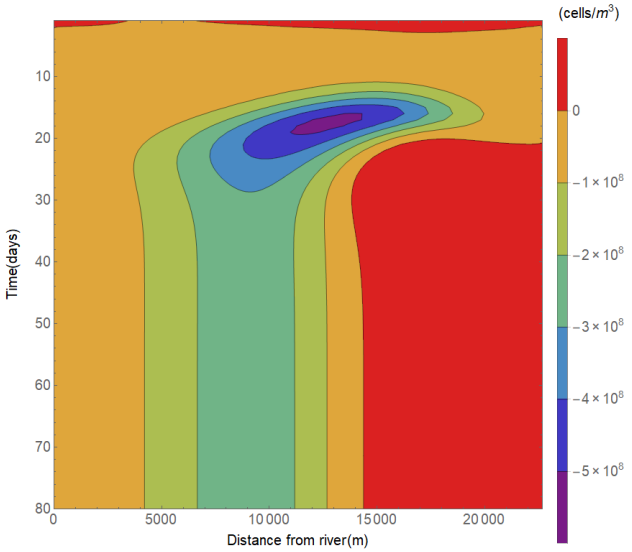

(e) As (b), but for the difference with the reference experiment.

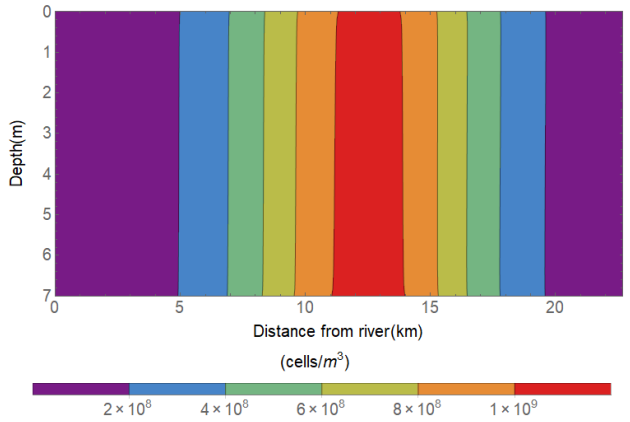

(c) The phytoplankton concentration on the 50th day, versus depth and distance from the river.

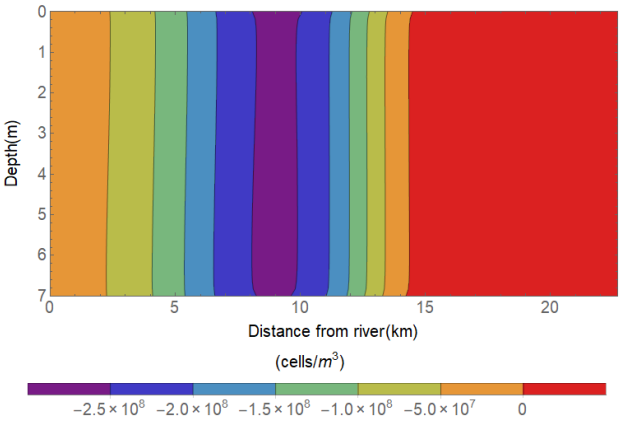

(f) As (c), but for the difference with the refernce experiment.

Figure 8: The results of the experiment with a diurnal cycle of intensity, where the average value is taken of the values at noon and midnight (and Q=10 m^3 s^{-1}).

3.4 Parabolic distribution of vertical eddy diffusivity and vertical eddy viscosity in combination with varying light intensity

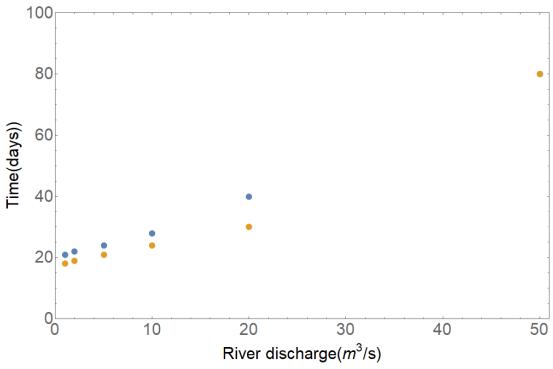

(a)The day at which the phytoplankton reaches his maximum amount in the estuary, for different cases of river discharge . For Q=50 m^3 s^{-1}, the bloom hasn't reached a steady state after 80 days.

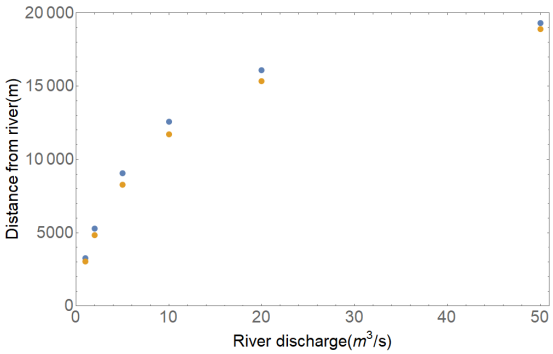

(b) The longitudinal location of the maximum depth-integrated phytoplankton concentration, on the 50th day of the simulation, for different cases of river discharge.

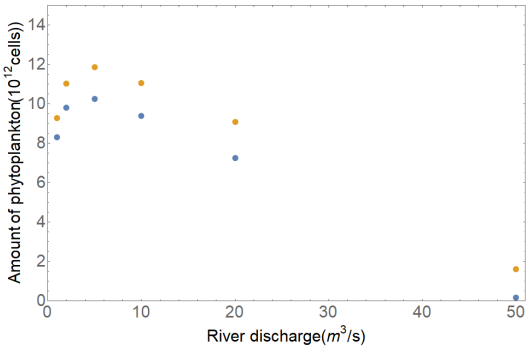

(c) The total amount of phytoplankton in the estuary, on the 50th day of the simulation, for different cases of river discharge.

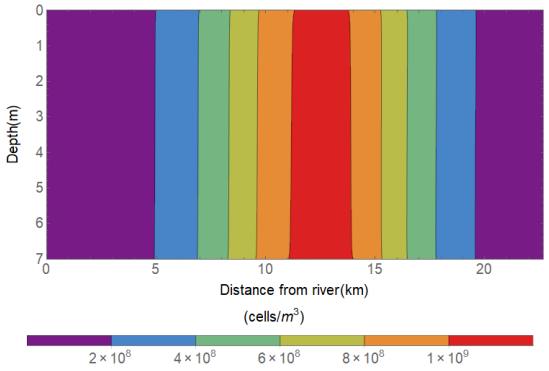

(d)The phytoplankton concentration on the 50th day of the simulation, versus depth and distance from river, for the experiment, and Q=10 m^3 s^{-1}.

Figure 9: The results for including both a parabolic vertical distribution of vertical eddy viscosity and vertical eddy diffusivity, and a diurnal cycle of light intensity. The blue dots represent the experiments, while the orange dots represent the reference experiments.

Figure 9 displays the results concerning varying light intensity in combination with a parabolic vertical distribution of vertical eddy viscosity and eddy diffusivity.

Figure 9(a) illustrates the timing of the phytoplankton blooms. For every case of river discharge, the bloom reaches his maximum value some days later than in the reference experiment. Figure 9(b) shows the longitudinal location of the maximum phytoplankton concentration, on the 50th day of the simulation. The maximum concentration is shifted seawards compared to the reference experiment. Figure 9(c) shows the total amount of phytoplankton in the estuary, on the 50th day of the simulation. It is observed that the values are always significantly lower than those in the reference experiment. Figure 9(d) displays the phytoplankton concentration on the 50th day, versus depth and distance from the river, and Q=10

m^3 s^{-1}. There is no vertical structure visible here. This holds true for every case of river discharge.

3.5 The role of tidal flow

Plots of the output of the model are made, where the average value is taken of measurements four times a day, to cover all stages of the tide, and placed in Figure 10. The observed patterns are not similar to those of the reference case. Figure 10(a) shows the total amount of phytoplankton for every point of time. One can see that no real bloom occurs, the concentrations of phytoplankton only triplicate compared to their starting value, instead of increasing by a factor 100, as was observed in the reference case. The maximum amount of phytoplankton occurs at the 7th day.

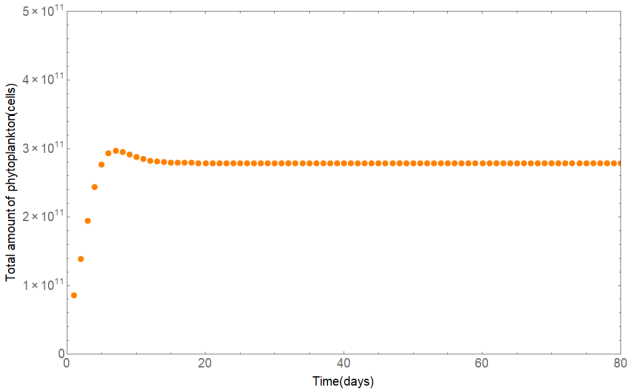

(a) The total amount of phytoplankton versus time.

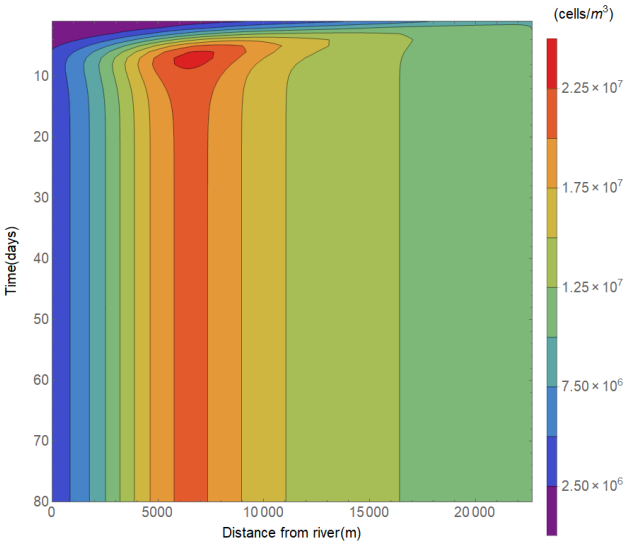

(b) The depth-averaged phytoplankton concentration, versus time and distance from the river.

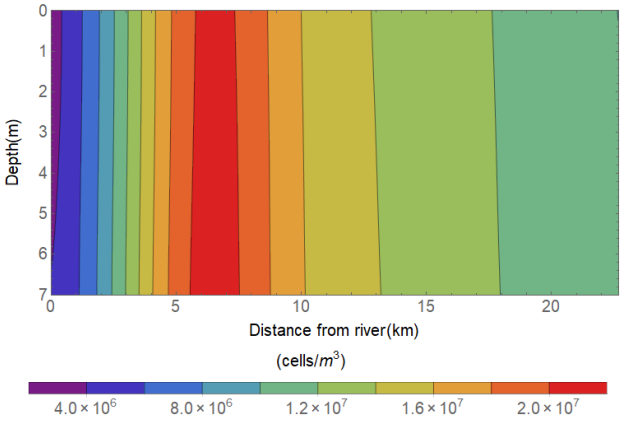

(c)The phytoplankton concentration on the 50th day, versus depth and distance from the river.

Figure 10: The results of the experiment with explicit tidal flow (and Q=10 m^3 s^{-1}).

Figure 10(b) illustrates the depth-averaged phytoplankton concentration, versus time and distance from the river. The highest concentrations of phytoplankton, in the steady situation, can be found 7 kilometres from the river mouth. Figure 10(c) displays the phytoplankton concentration on the 50th day, versus depth and distance from the river. No vertical structure in the phytoplankton concentration is observed here.

4 Discussion

In this section the observed patterns will be discussed, and, if possible, explained. Before starting to discuss this, it is investigated what limits the growthrate $\mu(N, I)$ of phytoplankton, for later reference. In the reference experiment, will the nutrients vary between 2.5 and 0.1 mmol/m^3 (as observed in the results), while the light, when ignoring the shading effect (the part $-k_{phyto}\int_o^z P(t,\theta)d\theta$ in equation 4), varies between 400 and 290 µmole photons m^{-2} s^{-1} (as calculated from equation 4). So $\frac{N}{H_N+N}$ will vary between 0.83 and 0.17, while $\frac{I}{H_I+I}$ varies between 0.95 and 0.94. Obviously, the value for the nutrient-limitation is always lower than the value for light-limitation, so the growthrate is nutrient-limited everywhere in the first weeks of the experiment. When there is sufficient phytoplankton, the shading of the phytoplankton starts to play a role, and this calculation does not hold true anymore.

4.1 Parabolic distribution of vertical eddy diffusivity and vertical eddy viscosity

First, as mentioned in 3.2, the timing of the phytoplankton blooms hardly changes due to the changed eddy viscosity and eddy diffusivity, if one looks at the total amount of phytoplankton in the estuary. This is because the observed deviations of 1% are too small to cause the bloom to shift.

The second interesting part is the lower value of phytoplankton in the estuary. The evolution in time of the total amount of phytoplankton is calculated by integrating equation 1 over the full domain. Some terms cancel (when assuming P is uniform in the vertical), and the following terms are left:

$$\int_V \frac{\partial P}{\partial t} dV = \int_V (\mu - m) P dV + Q(P_s - P_r) + \int_0^L \frac{H}{b}\frac{\partial}{\partial x}(\kappa_H b \frac{\partial P}{\partial x})dx. \qquad (20)$$

The term $Q(P_s - P_r)$ is independent from κ_ν and doesn't play a role. The last term is the horizontal diffusion of plankton to(of from) the sea and river. This is estimated to be small too. So the term investigated is $\int_V (\mu - m)PdV$. This term represents the difference between the growth rate and specific loss rate, times the phytoplankton concentration.

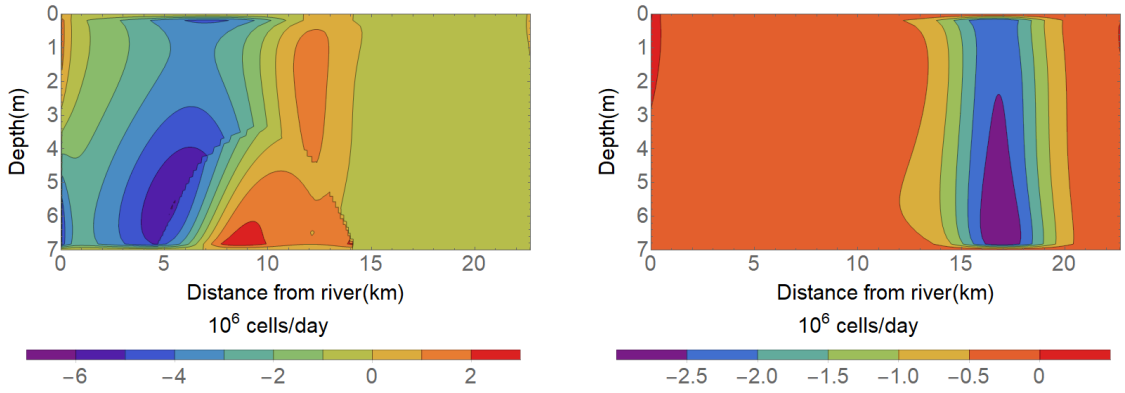

(a) (b)

Figure 11: (a) The difference between the experiment with a parabolic distribution of the eddy viscosity and eddy diffusivity and the reference experiment, in the total specific growth of phytoplankton, on the 50th day of the simulation, for Q=10 m^3 s^{-1}. (b) as (a), but for the 10th day of the experiment.

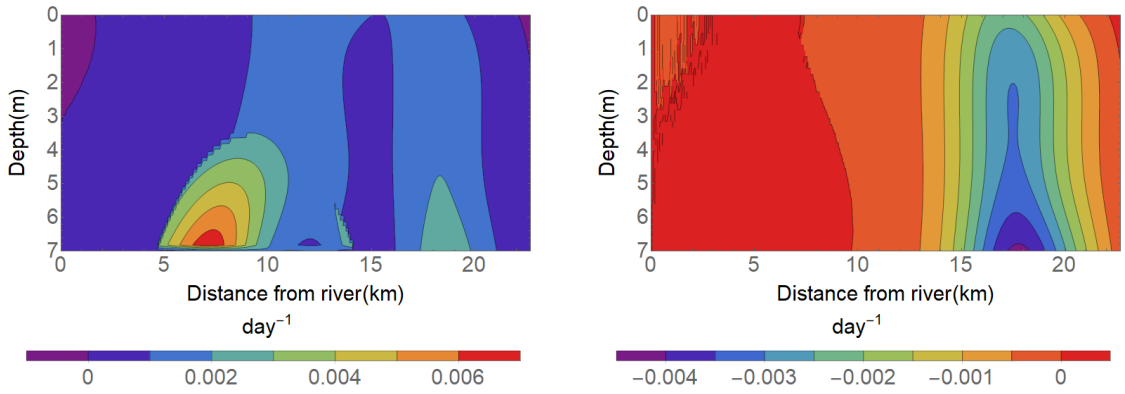

(a) (b)

Figure 12: (a) The difference between the experiment with a parabolic distribution of the eddy viscosity and eddy diffusivity and the reference experiment, in the growthrate of phytoplankton per day, on the 50th day of the simulation, for Q=10 m^3 s^{-1}.(b) as (a), but for the 10th day of the experiment.

More loss isn't an option, because the specific loss rate is a fixed value. So the second factor investigated the term $\int_V \mu P dV$, which we call "total specific growth". When looking at the absolute value of the specific growth, on the 50th day of the simulation, as shown in figure 11(a), there is less specific growth. This can be due to a lower value of μ, or just because the phytoplankton concentration is lower. A plot of μ is made and placed in figure 12(a). As one can see, it doesn't have a lower value, but a higher value to the contrary. This is due to a higher concentration of nutrients (because there is less used), as one can see in figure 13(a).

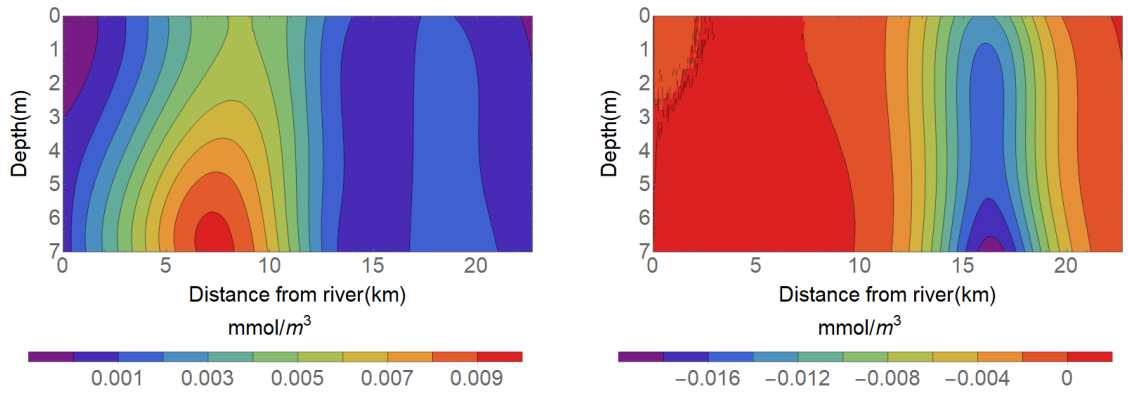

(a) (b)

Figure 13: (a) The difference in nutrient concentration between the experiment with a parabolic distribution of the eddy viscosity and eddy diffusivity and the reference experiment, on the 50th day of the simulation, for Q=10 m^3 s^{-1}. (b) as (a), but for the 10th day of the simulation.

So, the lower concentration phytoplankton is due to less total specific growth ($\int_V \mu P dV$), what is due to a lower concentration phytoplankton, and should be caused by factors during the upcoming of the bloom. They are investigated now. When looking at the growthrate during the start of the bloom (figure 12(b) gives the value at the 10th day), one can see that the growthrate after the most intense part of the bloom (that is around 18 kilometres from the river mouth) is lower, and because of that the total growth is lower too (figure 11(b). This is caused by a lower value of nutrients at this location (as visible in figure 13(b), light limitation plays no role here yet). When integrating equation 2 over the full domain (and assuming N is constant in the vertical), the following terms do not cancel:

$$\int_V \frac{\partial N}{\partial t} dV = \int_V (\epsilon m - \mu)\alpha P dV + Q(N_s - N_r) + \int_0^L \frac{H}{b}\frac{\partial}{\partial x}(\kappa_H b \frac{\partial N}{\partial x})dx. \quad (21)$$

The term $Q(N_s - N_r)$ is independent of κ_ν. Which of the other two terms is responsible for the lower nutrient concentration hasn't become clear. So to conclude: due to less total specific growth, the phytoplankton will never reach the same value as in the reference experiment, so the total specific growth stays at a lower level, and the phytoplankton ends up in a lower equilibrium concentration.

This explains the lesser amount of phytoplankton cells in the estuary, and why after the peak of the bloom the concentration is lower (because from the start, there grows less plankton there). Why also before the bloom the concentration phytoplankton is lower isn't explained by this. This second place where is less phytoplankton starts to occur around the 20th day of the simulation. The exact reason why this happens isn't found. But it is stressed the differences are small and probably there can't be found a clear physical reason for this. These differences should become larger when the sinking velocity of phytoplankton is larger, and more vertical structure in the phytoplankton concentration arises.

The last pattern discussed is the vertical structure: where the phytoplankton has a lower concentration, the deviations occur at the surface and in the lower

half of the water column. Already at the start, the difference in growthrate is the highest at the bottom. This is predominantly due to a lower nutrient concentration, as mentioned before, and visible in figure 13(b). So, from this point onwards, the phytoplankton concentration close to the bottom is lower, because in the beginning less growth existed there. The lower concentration at the surface existed since the start of the bloom too, but isn't caused by a lower nutrient concentration. The reason for this pattern isn't found.

4.2 Varying light intensity

First, the smaller size of the bloom will be discussed. As mentioned before, in the reference experiment light limitation doesn't play a role during formation of the bloom. This explains why the total amount of phytoplankton is smaller compared to the reference case in this experiment. The light intensity goes to zero around midnight, so here the growth will be light-limited. At noon, the light intensity duplicates, but this has no effect on the growthrate of phytoplankton, because there is no light limitation anymore, even for the reference light intensitiy. So there appears an extra limitation (which is predominantly present during formation of the bloom) on the growthrate, during the night, which causes a lower net value of the growthrate (see figure 14 for a plot of this phenomenon). This causes the lower concentration phytoplankton.

When the bloom becomes big enough to let the shading effect become relevant, the increased light intensity around noon causes a higher growthrate, but this effect is smaller than the previously described one. So the overall growthrate is smaller, particularly during the formation of the bloom, which causes the smaller size of the phytoplankton bloom.

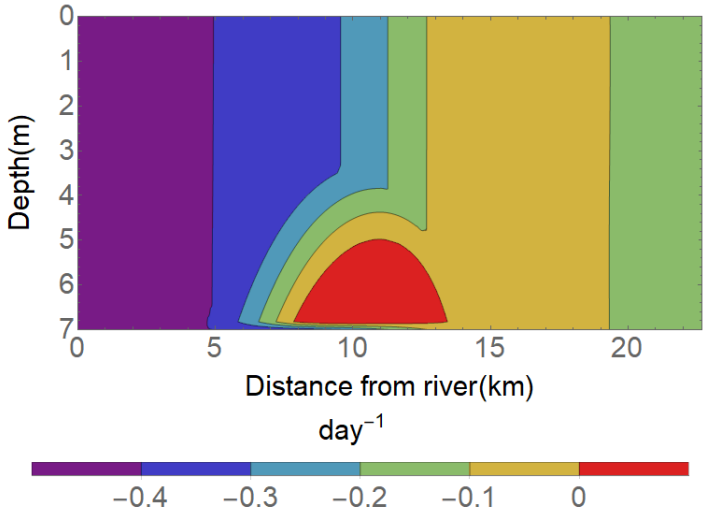

Figure 14: The difference between the experiment with varied light intensity and the reference experiment, in the growthrate of phytoplankton, on the 50th day of the simulation, for Q=10 m^3 s^{-1}. The showed values are averaged over the values at noon and midnight.

The next thing discussed is the location of the bloom. The limitation on the growthrate due to the decreased light intensity happens predominantly in the upper reach of the estuary, because most of the growth takes place here, because of the high nutrient concentration (remember the nutrients are supplied by the river). In the lower reach exists a small region where is more phytoplankton, this is due to the fact that less nutrients are used at the beginning of the estuary, so the nutrient concentration is higher in the middle of the estuary, and there is more growth possible here. This is the reason why the bloom shifts seawards.

Also, the timing of the bloom is explained by the lower value of the growthrate: due to the extra limitation, the phytoplankton has less time per day to grow, so it will take more time to reach his maximum.

The last thing needed to explain is the absence of vertical structure in the phytoplankton concentration by varying the light intensity. Vertical structure, caused by varying the light intensity, can possibly arise when the growthrate in the lower layer is limited due to absence of light, while in the upper layer sufficient light is present, so at different depths different growthrates and thus different concentrations phytoplankton arise. This is the case during low incident light intensity, so at certain times of the day, and at locations with high phytoplankton concentrations (due to the shading effect). But apparently this isn't enough to cause vertical structure in the phytoplankton concentration. When looking at the size of the terms in equation 1, the vertical diffusion ($\frac{\partial}{\partial z}(\kappa_\nu \frac{\partial P}{\partial z})$) is of the same order of magnitude as the specific growth (μP) (specific growth has a maximum value of 4000 cells/(second m^3), while vertical diffusion can have a value of 6000 cells/(second m^3)). So due to the strong mixing in the vertical, no vertical structure in the phytoplankton concentration arises.

4.3 Parabolic vertical eddy diffusivity and vertical eddy viscosity in combination with varying light intensity

The results from this section have many similarities with the results from only varying the light intensity. This is because the variations caused by the varying light intensity are larger (by a factor of at least 10) than those caused by the parabolic eddy viscosity and eddy diffusivity. So, all observed changes are due to the diurnal cycle of the light, and are thus discussed in the previous section.

The best way to continue this discussion would be to compare both the reference experiment and these experiments with measurements of phytoplankton concentrations in the Taw, and see which model is the closest to the real values. But these measurements don't exist. *Maier* [2012] used field data for his research, but he measured mainly chlorophyll a, what is a good indication for the presence of phytoplankton, but it is hard to translate this to an exact number of cells of phytoplankton. So this comparison can unfortunately not be made.

4.4 The role of tidal flow

The reproduced results here are not realistic: when adding tidal flow, there should still form a bloom similar to the bloom in the reference experiment. But here, the size of the bloom is much smaller: by factor 100. So something is going wrong here. The problem turns out to lay in the boundary conditions: nutrients and phytoplankton advect through the estuary on small timescales (a couple of hours), due to the tidal flow, so P and N will vary in the longitudinal direction. But at $x = L$, constant boundary conditions are applied. This leads to large horizontal gradients of nutrients and phytoplankton, which is not physically. To solve this problem, time-dependent boundary conditions should be used.

4.5 Model limitations

The model used for this experiment is a highly idealised model. This means it is far from complete, and several assumptions have been made. The most important ones will be mentioned here.
First, only one species of phytoplankton is used. But there are thousands of species of phytoplankton [*Falkowski*, 2012], and all of them react differently to light, temperature and nutrients, a fact that is not taken into account by this model. The same is true for nutrients: this is modelled as one variable, but in fact there are different sorts of nutrients too: phosphate, nitrate and other ones. There can be plenty of one nutrient, but if one other is absent, the phytoplankton still can't survive, a fact this model can't reproduce. Even more, different species of phytoplankton have different needs for nutrients.
Secondly, the model only works with two spatial coordinates, but in nature there are of course three dimensions. So there is no space for transverse factors in this model, which can however be important. For instance, this model gives no information about the transverse distribution of the plankton.
Subsequently, the model takes the water depth as a constant, and the width of the estuary is exponentially increasing. No estuaries like this exist in nature: in reality the coastline is always complicated, and the bottom too. On top of that, in estuaries often channels separated by sandy shoals exist, which make the geography even more complicated. It is stressed that the model never tried to cover these features, because it is an idealised model and not a complex model, which is specifically designed to gain more fundamental knowledge about the different factors influencing phytoplankton blooms.
Next, temperature doesn't play a role in the used model. But the water temperature gives restrictions to the growth of phytoplankton (see for instance *Eppley* [1972]), and should be covered too.
Finally, a lot of parameters are taken constant in this model, but these are simplifications and should vary in space and time. We will mention the most important ones here and explain why this is an approximation:

- salinity(s) is a taken constant in time and in the vertical. The justification for taking it constant in the vertical is that the estuary is well-mixed in this dimension. Taking it constant in time is an approximation by all means: when involving tides, the sea water flows upstream and downstream, and the salinity

should follow. But the model does not govern this.

- The vertical eddy diffusion coefficient and vertical eddy viscosity have now been taken parabolic, but they strongly depend on the water flow velocities, and so they do depend on the tides as well (and on top of that, the degree of stratification plays in important role too).
- The background turbidity (k_{bg}) is taken constant. But the turbidity is predominantly generated by eroding sediment from the bottom [*Dyer*, 1997], and thus its behaviour is a strong function of flow velocity.

All these factors give limitations at the point to which one can extrapolate the conclusions of this experiment. Further research is needed to study the influence of these factors.

5 Conclusions

In this study, the deformation of phytoplankton blooms in well-mixed estuaries is investigated with an idealised model. One important finding is that if vertical profiles of vertical eddy viscosity and vertical eddy diffusivity are changed from constants to parabolic distributions, P values become about 1% smaller, in particular in the lower half of the estuary. This is because during formation of the bloom, less nutrients are present in the estuary. The reason for this is not found.
Second, if a daily cycle of incident light intensity is used instead of a constant value, the P values become about 15% smaller, and it takes the bloom more time to reach is maximum size. The reason is that the growthrate of phytoplankton is not light-limited in the reference case, but it becomes light-limited during low light intensities in the experiment. So an extra limitation on the growthrate appears.
Third, if vertical profiles of vertical eddy viscosity and vertical eddy diffusivity with a diurnal cycle of incident light intensity are combined, no new patterns are found.
Finally, doing an experiment with explicit tidal flow instead of a subtidal flow profile needs proper boundary conditions.

A The derivation of the longitudinal velocity for subtidal flow, with the parabolic distribution of A_v involved (equation18)

The starting point for this derivation is the momentum balance for an estuary [*Hansen and Rattray*, 1965], as stated in 2.1. The meaning of the symbols used are described earlier in table 1. These equations read:

$$0 = -\frac{1}{\rho_0}\frac{\partial p}{\partial x} + \frac{\partial}{\partial z}(A_\nu \frac{\partial u}{\partial z}), \tag{22}$$

$$\frac{\partial p}{\partial z} = \rho g, \tag{23}$$

$$\rho = \rho_0 + \beta s, \tag{24}$$

With corresponding boundary conditions:

$$A_\nu \frac{\partial u}{\partial z} = 0 \quad \text{at} \quad z = 0, \tag{25}$$

$$u = 0 \quad \text{at} \quad z = H - z_0, \tag{26}$$

$$\int_0^{H-z_0} u \quad dz = \frac{Q}{b}. \tag{27}$$

To solve equation 22, the first step is to get an expression for $\frac{\partial p}{\partial x}$. For this, first, the solution of equation 23 is determined, which reads:

$$\frac{\partial p}{\partial z} = \rho g, \tag{28}$$

$$\frac{\partial p}{\partial x} = gz\beta\frac{\partial s}{\partial x} + g\rho_0\frac{\partial \eta}{\partial x}. \tag{29}$$

For the last step is used that we can write $p_0 = \rho_0 \eta g$, where η is the deviation of the water surface from its reference position. Inserting this result in 22 yields:

$$g\frac{\partial \eta}{\partial x} + \frac{g\beta}{\rho_0}\frac{ds}{dx}z = \frac{\partial}{\partial z}(A_\nu \frac{\partial u}{\partial z}). \tag{30}$$

When A_ν is taken constant and $z_0 = 0$, the solution of these equations is the equation used by *Liu and de Swart* [2015](details are given in *Hansen and Rattray* [1965]):

$$u(x,t) = \frac{3Q}{2b(x)H}(1 - (\frac{z}{H})^2) + \frac{gH^3\beta}{48\rho_0 A_\nu}\frac{ds}{dx}(1 - 9(\frac{z}{H})^2 + 8(\frac{z}{H})^3) \tag{31}$$

For a parabolic vertical profile of A_ν (17):

$$A_\nu(z) = \alpha z(H - z). \tag{32}$$

Equation 30

$$g\frac{\partial \eta}{\partial x} + \frac{g\beta}{\rho_0}\frac{ds}{dx}z = \frac{\partial}{\partial z}(A_\nu \frac{\partial u}{\partial z}). \tag{33}$$

is integrated form level z to the surface, and the boundary condition at z=0 is applied. This yield:

$$\frac{\partial u}{\partial z} = \frac{\partial \eta}{\partial x}\frac{g}{\alpha}\frac{1}{H-z} + \frac{g\beta}{\rho_0}\frac{ds}{dx}\frac{1}{2\alpha}\frac{z}{H-z}. \tag{34}$$

Integrating again from z to the bottom, and using the boundary condition at the bottom, gives:

$$u = -\frac{\partial \eta}{\partial x}\frac{g}{\alpha}\log(\frac{H-z}{z_0}) + \frac{g\beta}{\rho_0}\frac{ds}{dx}\frac{1}{2\alpha}(-H\log(\frac{H-z}{z_0}) + H - z - z_0). \tag{35}$$

With the last boundary condition, one can get the expression for $\frac{\partial \eta}{\partial x}$. So integrating one more time, now over the full depth of the water column, and applying boundary condition 27, results in:

$$\frac{\partial \eta}{\partial x} = \frac{1}{2}\frac{\beta}{\rho_0}\frac{ds}{dx}\left(H + \frac{\frac{1}{2}(H-z_0)^2}{z_0 - H + H\log(\frac{H}{z_0})}\right) - \frac{Q\alpha}{gb\big(z_0 - H + H\log(\frac{H}{z_0})\big)}. \tag{36}$$

So the final solution is found by putting this back into (35):

$$u(x,t) = \frac{Q}{bH}\frac{\log(\frac{H-z}{z_0})}{\log(\frac{H}{z_0}) + \frac{z_0}{H} - 1} + \frac{g\beta}{\rho_0}\frac{ds}{dx}\frac{1}{2\alpha}\left(\frac{\log(\frac{H-z}{z_0})\frac{1}{2}(H-z_0)^2}{z_0 - H + H\log(\frac{H}{z_0})} + H - z - z_0\right). \tag{37}$$

B The tidal velocities

The tidal velocities are:

$$u(x,z,t) = |\hat{u}|\cos(\omega t - \phi_u), \tag{38}$$
$$w(x,z,t) = |\hat{w}|\cos(\omega t - \phi_w), \tag{39}$$

where

$$\phi_u = \arg(\hat{u}), \tag{40}$$
$$\phi_w = \arg(\hat{w}), \tag{41}$$
$$\hat{u} = \upsilon p_0(z) f(x), \tag{42}$$
$$\hat{w} = \upsilon q_0(z) g(x), \tag{43}$$

where

$$\upsilon = \frac{ig}{\omega} A_{mz} \kappa_0, \tag{44}$$
$$p_0 = 1 - \frac{\cosh(\gamma z)}{\cosh(\gamma H)}, \tag{45}$$
$$f(x) = e^{\frac{L-x}{2L_b}} \left(\frac{\kappa_0 \sin(d_0 x)}{d_0 \cos(d_0 L) + \frac{1}{2L_b}\sin(d_0 L)} \right), \tag{46}$$
$$q_0 = 1 - \frac{z}{H} + \frac{1}{\gamma H}\left(\frac{\sinh(\gamma z) - \sinh(\gamma H)}{\cosh(\gamma H)} \right), \tag{47}$$
$$g(x) = e^{\frac{L-x}{2L_b}} \kappa_0 H \left(\frac{\frac{1}{2L_b}\sin(d_0 x) + d_0 \cos(d_0 x)}{d_0 \cos(d_0 L) + \frac{1}{2L_b}\sin(d_0 L)} \right), \tag{48}$$
$$d_0^2 = \kappa_0^2 - \frac{1}{4L_b^2}, \tag{49}$$
$$\kappa_0^2 = \frac{\omega^2}{gH}\left(\frac{1}{1 - \frac{1}{\gamma H}\tanh(\gamma H)} \right), \tag{50}$$
$$\gamma = \sqrt{\frac{-i\omega}{A_\nu}}. \tag{51}$$

Here, ω is the frequency of the tide, and A_{mz} is the tidal amplitude. The period of the tide is chosen at 12 hours (in reality, this is a slightly different value, but to keep things simple we chose this number). So the value of ω becomes $\frac{2\pi}{12\times 3600} = 1.45 \times 10^{-4}$ s^{-1}. In the case of the Taw estuary, the tidal amplitude is approximately 3.5 meter [*WillyWeather*, 2018]. When inserting this value in the formula, the velocities become weaker than observed [*Pethick*, 2007]. This is because the equations are solved for boundary conditions which imposed zero velocity at x=0, what doesn't hold for the Taw estuary. To solve this problem, and get the observed velocities of 1 m s^{-1}, A_{mz} is chosen at 7.5 meters (Of course this is not realistic for a water depth of 7 meters, but it is needed to get the right velocities). All other used symbols are previously defined.

References

Azevedo, I., A. Bordalo, and P. Duarte, Influence of freshwater inflow variability on the douro estuary primary productivity: a modelling study., *Ecological Modelling*, *272*, 1–15, 2014.

Burchard, H., and R. Hetland, Quantifying the contributions of tidal straining and gravitational circulation to residual circulation in periodically stratified tidal estuaries., *Journal of Physical Oceanography*, *40*, 12431262, 2010.

Carstensen, J., R. Klais, and J. E. Cloern, Phytoplankton blooms in estuarine and coastal waters: Seasonal patterns and key species., *Estuarine, Coastal and Shelf Science*, *162*, 98–109, 2015.

Dugdale, R., F. Wilkerson, A. Parker, A. Marchi, and K. Taberski, Riverflow and ammonium discharge determine spring phytoplankton blooms in an urbanized estuary., *Estuarine, Coastal and Shelf Science*, *115*, 187–199, 2012.

Dyer, K. R., *Estuaries: A Physical Introduction*, 2 ed., John Wiley and Sons, Baffins Lane, Chichester, West Sussex P019 IUD, England, 1997.

Ensing, E., H. E. de Swart, and H. M. Schuttelaars, Sensitivity of tidal motion in well-mixed estuaries to cross-sectional shape, deepening, and sea level rise., *Ocean Dynamics*, *65*, 933–950, 2015.

Eppley, R. W., Temperature and phytoplankton growth in the sea., *Fisheries Bulletin NOAA*, *70*, 1063–1085, 1972.

Falkowski, P., The power of plankton., *Nature*, *483*, 2012.

Fischer, H. B., *Mixing in Inland and Coastal waters*, 1 ed., Academic Press, Inc, San Diego, California, 1979.

Hansen, D. V., and M. Rattray, Gravitational circulation in straits and estuaries., *Journal of Marine Research*, *23*, 104–122, 1965.

Helder, W., and P. Ruardij, A one-dimensional mixing andflushing model of the ems-dollard estuary: calculation of time scales at different river discharges., *Netherlands Journal of Sea Research*, *15*, 293–312, 1982.

Huisman, J., N. Thhi, D. Karl, and B. Sommeijer, Reduced mixing generates oscillations and chaos in the oceanic deep chlorophyll maximum., *Nature*, *439*, 322–326, 2006.

Liu, B., and H. E. de Swart, Impact of river discharge on phytoplankton bloom dynamics in europhic estuaries: A model study., *Journal of Marine Systems*, *152*, 64–74, 2015.

Maier, G., A high resolution temporal study of phytoplankton bloom dynamics in the eutropic taw estuary(sw england), *Science of the Total Environment*, *434*, 28–239, 2012.

May, C., J. Koseff, L. Lucas, J. Cloern, and D. Schoellhamer, Effects of spatial and temporal variability of turbidity on phytoplankton blooms., *Marine Ecology Progress Series*, *254*, 111–128, 2003.

Munk, W., and E. Anderson, Notes on a theory of the thermocline., *Journal of Marine Research*, *7*, 276–295, 1948.

Naithani, J., B. de Brye, E. Buyze, W. Vyverman, V. Legat, and E. Deleersnijder, An ecological model for the scheldt estuary and tidal rivers ecosystem: spatial and temporal variability of plankton, *775*, 2016.

NASA, Importance of phytoplankton, `https://earthobservatory.nasa.gov/Features/Phytoplankton/page2.php`, [Online; accessed 5-March-2018], 2010.

NOAA, What are phytoplankton?, `https://oceanservice.noaa.gov/facts/phyto.html`, [Online; accessed 20-March-2018], 2017.

Pethick, J., The taw-torridge estuaries: Geomorphology and management report to taw-torridge estuary officers group., *Unesco Biosphere Reserve*, 2007.

Popovich, C., and A. Gayoso, Effect of irradiance and temperature on the growth rate of thalassiosira curviseriata takano (bacillariophyceae), a bloom diatom in bahia blanca estuary (argentina)., *Journal of Plankton Research*, *21*, 11011110, 1999.

Sarthou, G., K. Timmermans, and S. Blain, Growth physiology and fate of diatoms in the ocean: a review., *Journal of Sea Research*, *53*, 25–42, 2005.

Sin, Y., R. Wetzel, and I. Anderson, Spatial and temporal characteristics of nutrient and phytoplankton dynamics in the york river estuary, virginia: analyses of long-term data., *Estuaries and Coasts*, *22*, 260–275, 1999.

Warner, J., W. Geyer, and J. Lerczak, Numerical modeling of an estuary: a comprehensive skill assessment., *Journal of Geophysical Research*, *110*, 2005.

WillyWeather, River Taw Entrance Tide Times and Heights, `https://tides.willyweather.co.uk/sw/devon/river-taw-entrance.html`, [Online; accessed 24-May-2018], 2018.